

Characterization and modeling of volumetric and mechanical properties for step and flash imprint lithography photopolymers

Matthew Colburn, Itai Suez, Byung Jin Choi, Mario Meissl, Todd Bailey, S. V. Sreenivasan, John G. Ekerdt, and C. Grant Willson^{a)}

Texas Materials Institute, The University of Texas at Austin, Austin, Texas 78712

(Received 1 June 2001; accepted 1 October 2001)

Step and flash imprint lithography (SFIL) is an alternative approach to high-resolution patterning based on a bilayer imprint scheme. SFIL utilizes the *in situ* photopolymerization of an oxygen etch resistant monomer solution in the topography of a template to replicate the template pattern on a substrate. The SFIL replication process can be affected significantly by the densification associated with polymerization and by the mechanical properties of the cured film. The densities of cured photopolymers were determined as a function of pendant group volume. The elastic moduli of several photopolymer samples were calculated based on a Hertzian fit to force–distance data generated by atomic force microscopy. The current SFIL photopolymer formulation undergoes a 9.3% (v/v) densification. The elastic modulus of the SFIL photopolymer is 4 MPa. The densification and the elastic modulus of the photopolymer layer can be tailored from 4% to 16%, and from 2 to 30 MPa, respectively, by changing the structure of the photopolymer precursors and their formulation. The complex interaction among densification, mechanical properties (elastic modulus and Poisson's ratio) and aspect ratio (height:width) was studied by finite element modeling. The effect of these parameters on linewidth, sidewall angle, and image placement was modeled. The results indicate that the majority of densification occurs by shrinkage in the direction normal to the substrate surface and that Poisson's ratio plays a critical role in defining the shape of the replicated features. Over the range of material properties that were determined experimentally, volumetric contraction of the photopolymer is not predicted to adversely affect either pattern placement or sidewall angle. © 2001 American Vacuum Society. [DOI: 10.1116/1.1420199]

I. INTRODUCTION

Step and flash imprint lithography (SFIL) is a patterning process utilizing photopolymerization to replicate the topography of a template onto a substrate.^{1,2} Polymerization, however, is often accompanied by densification. The interaction potential between photopolymer precursors undergoing free radical polymerization changes from Van der Waals' to covalent. The average distance between the molecules decreases and causes volumetric contraction. Densification of the SFIL photopolymer (the etch barrier) may affect both the cross sectional shape of features and the placement of relief patterns. Finite element modeling (FEM) makes it possible to explore the influence of densification and mechanical properties on changes in the placement and in the geometry of the replicated features. The densification and elastic modulus of prospective etch barrier candidates have been characterized and were used as the basis for the physical properties in FEM simulation.

II. EXPERIMENTAL METHODS

The densities of the photopolymers were determined by Archimedes' principle. In these experiments, dry samples T_1 were first weighed in air. Then the samples T_2 were weighed while submerged in a fluid of known density ρ_{liq} . Equation

(1) relates the density of the sample ρ_{sample} to the difference in the measured weights. The volumetric change was calculated using Eq. (2):

$$\rho_{\text{sample}} = \rho_{\text{liq}} \left(\frac{T_1}{T_2} \right), \quad (1)$$

$$\Delta V = \left(\frac{\rho_{\text{polymer}} - \rho_{\text{monomer}}}{\rho_{\text{polymer}}} \right). \quad (2)$$

The elastic modulus of the etch barrier films was characterized by nanoindentation on a Thermomicroscope CP Research atomic force microscope (AFM) equipped with an Ultralever B tip which has a spring constant of 0.4 N/m. The calibration procedure prescribed by Thermomicroscopes for the force–distance analysis was performed on each Ultralever B tip.³ In the nanoindentation process, the AFM cantilever is actuated toward the sample a distance z . When the tip comes in contact with the sample, the cantilever is deflected a distance d . The force imparted on the sample is directly proportional to this deflection by the spring constant k of the cantilever. This force results in the indentation of the sample to a depth δ . The cantilever travel is equal to the deflection plus the indentation depth ($z = d + \delta$).

The contact mechanics of a tip impinging on a surface have been extensively studied.^{4–6} Several models were considered, but the Hertzian model has proved to be more robust for these samples and was used to analyze all force–distance data.⁴ In the Hertzian model, the material is assumed to be

^{a)}Author to whom correspondence should be addressed; electronic mail: willson@che.utexas.edu

have isotropically and have no attractive forces that distort the contact area between the tip and the substrate, and the indenter is assumed to have a spherical tip of radius R . Under these assumptions, the observed force F obeys the following equation:

$$F = (K^2 R \delta^3)^{1/2}, \quad (3)$$

where

$$\frac{1}{K} = \frac{3}{4} \left(\frac{1 - \nu_s^2}{E_s} + \frac{1 - \nu_{\text{tip}}^2}{E_{\text{tip}}} \right),$$

ν is Poisson's ratio and E is the tensile modulus. Since the modulus of the AFM tip E_{tip} is much greater than the modulus of the samples E_s , the second part of the quotient is approximately zero. Linear regression of the force against $\delta^{3/2}$ yields a slope that is equal to $4E_s/(3(1-\nu_s^2))$. The elastic modulus can be calculated if Poisson's ratio is known. We have approximated this value at 0.35.

Solid models of the etch barrier layer in SFIL were developed using Pro/E[®], a commercially available computer aided design package, and analyzed using FEM techniques in Pro/E Mechanical[®]. The isotropic densification of the etch barrier was simulated using pseudocoefficients of thermal expansion (CTE) defined as the volumetric shrinkage of the etch barrier divided by 1 °C. A model was created at a reference temperature and assigned physical properties (E , ν , CTE). Rigid interfaces were modeled as fixed boundaries. The temperature of the model was modulated by 1 °C, which resulted in the defined isotropic volumetric contraction. The final state of each model was then compared to the model in the reference state. These models actually simulate a worst-case scenario in which the photopolymerization is completed isotropically in the reference state, then allowed to contract to the model state. Two sets of simulations were performed to identify the effect that pattern layout might have on pattern placement and the effects that etch barrier properties have on feature shape.

The pattern placement study was performed on the pattern shown in the top down view in Fig. 1(a). In the reference state, the features are 200 nm tall. The lines and boxes are separated by 100 nm. The boxes are 2 μm by 2 μm squares. The length of the central line that runs along the boxes is 7.6 μm long. The line that is perpendicular to the central line is 2.5 μm long. The base layer is 100 nm thick and the rigid boundary condition fixed at the bottom of the base layer. The top of the etch barrier was free. The modulus of the etch barrier was 1.6 MPa and Poisson's ratio was estimated at 0.3. The etch barrier densification is 10% (v/v). The motion of the 7.6 μm long centerline was analyzed at the base of the features for displacement motion in-plane with the substrate. This in-plane displacement magnitude was defined as shown below:

$$D_{\text{in-plane}} = \sqrt{\delta_x^2 + \delta_y^2}, \quad (4)$$

where δ_x and δ_y are orthogonal displacement vectors that are parallel to the substrate surface.

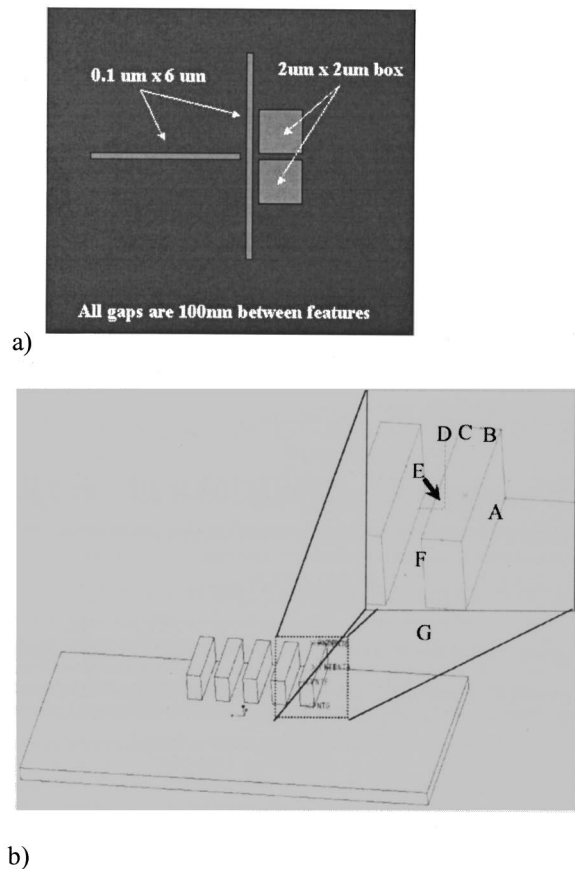


FIG. 1. (a) Pattern placement model. (b) Model used for the full factorial simulations.

The second set of simulations modeled the effect of the aspect ratio, Poisson's ratio, and elastic modulus on the geometry of dense features. The model system is shown in Fig. 1(b). A rigid bottom surface of base layer was used to simulate a transfer layer with a modulus much greater than that of the etch barrier. The reference points are labeled A–G. The displacements of these points were used to calculate the change in length, height, and sidewall. The sidewall angles were determined by the dot product of the vectors defined by the lines AE and AB, and lines AE and DE. A symmetric boundary condition was placed through the center of the model, halfway along the length of the features. The simulations were performed using a full factorial design of experiment on the 200 nm tall feature with linewidths of 100 nm, 500 nm, 1 μm , and 10 μm , and densifications of 3%, 6.0%, 11.5%, and 17%. The features had a length to width ratio of 10 and a 1:1 pitch (linewidth: line space) except for the 10 μm features which had a length to width ratio of 1:1. The base layer was 100 nm. The elastic modulus and Poisson's ratio were 1 MPa and 0.5, respectively.

In addition to the above simulations, Poisson's ratios of 0.3 and 0.4 were applied to models with densification of 6.0% and 11.5% and linewidths of 100 nm, 500 nm, and 1 μm . Also, 200 nm wide lines having a Poisson's ratio of 0.5 were simulated for densifications of 3% and 17%.

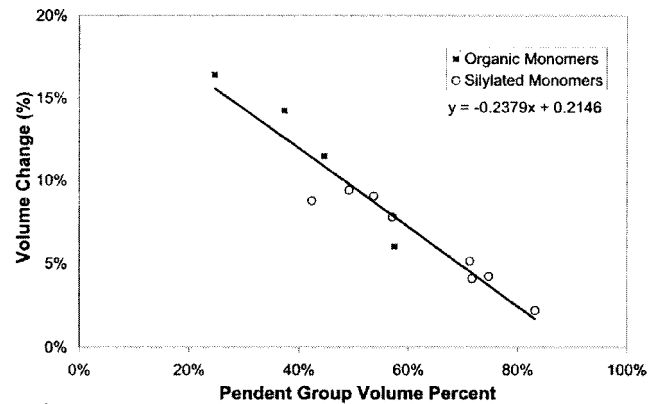
III. RESULTS

The effect of pendant group size on densification was investigated for a series of monomers that undergo free radical polymerization. Ethyl acrylate, butyl acrylate, hexyl acrylate, lauryl acrylate, 2-(acryloxyethoxy)trimethylsilane (SIA 0160, Gelest), (3-acryloxypropyl) dimethylmethoxysilane (SIA 0190, Gelest), (3-acryloxypropyl) methylbis(trimethylsiloxy)silane (SIA 0194, Gelest), ((3-acryloxypropyl)-tris(trimethylsiloxy)silane (SIA 0210, Gelest), acryloxytrimethylsilane (SIA 0320, Gelest), methacryloxyethoxytrimethylsilane (SIM 6481, Gelest), methacryloxypropyltris(trimethylsiloxy)silane (SIM 6487.6, Gelest), and ~ 900 molecular weight monomethacryloxypropyl terminated polydimethylsiloxane (MCR-M11, Gelest) monomer solutions were formulated with 1 mole % of 1,3-bis(3-methacryloxypropyl) tetramethyldisiloxane (SIB 1402.0, Gelest) and 1.6 mole % of 1:1 (w/w) mixture of bis(2,4,6-trimethylbenzoyl)-phenylphosphineoxide (Irgacure 819, Ciba) and 1-benzoyl-1-hydroxycyclohexane (Irgacure 184, Ciba); then cured under an N_2 purge. The incorporation of SIB 1402.0, a crosslinker, produces a solid sample that is easily handled.

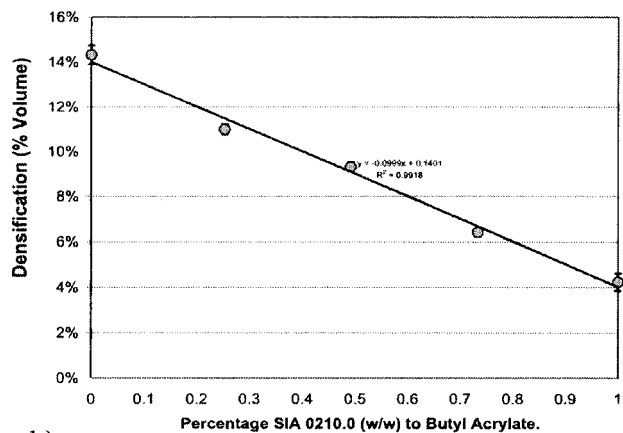
HyperChem[®] molecular dynamic simulations were utilized to determine the molecular volume (\AA^3) of four alkyl acrylates and the eight silylated monomers. The volumes of acrylic acid and methacrylic acid were simulated and their volumes were defined as the reactive volumes for the acrylic and methacrylic monomers, respectively. The pendant group volume for each monomer was defined as the volume of the monomer minus the reactive volume. A plot of the densification against the volume fraction of the pendant group is shown in Fig. 2(a). The densification of alkyl acrylate monomers () starts at 16.5% for ethyl acrylate and decreases with increasing pendant group volume to a value of 6% for lauryl acrylate. The densification of the silylated monomers () follows a trend similar to that of the organic monomers [Fig. 2(a)]. The pendant group volume effectively dilutes the effect of the densification caused by the generation of covalent bonds formed during photopolymerization of the acrylate.

Since the etch barrier is a blend of two principle components: butyl acrylate and SIA0210, it is necessary to study the effect that blending monomers has on the volumetric change. Butyl acrylate and SIA 0210 were mixed at 25% (w/w) intervals from 100% butyl acrylate to 100% SIA0210. 1% (w/w) SIB1402 and 3% (w/w) of the 1:1 mixture of Irgacure 819 and Irgacure 184 were added to these solutions. The resulting mixtures were cured, their densities measured, and their volume change calculated [Fig. 2(b)]. The system behaves ideally; there is no interaction present in this system. The densification of the current etch barrier formulation is 9.3% (v/v). It consists of 50% (w/w) *n*-butyl acrylate, 50% (w/w) SIA 0210, to which 5% (w/w) SIB 1402, and 3% (w/w) of 1:1 mixture of Irgacure 819 and Irgacure 184 were added.

The elastic moduli of prospective etch barrier components were evaluated by Hertzian fits to data gathered during the nanoindentation experiments. The modulus of SIM 6481 and



a)



b)

FIG. 2. (a) Volumetric contraction as a function of molecular volume (\AA^3). (b) Densification of 3-acryloxypropyl tris(trimethylsiloxy)silane and butyl acrylate blends.

methacryloxypropylpentamethyl disiloxane (SIM 6487, Gelest) were calculated to be 18.5 and 30 MPa, respectively. The moduli of ethyl acrylate, butyl acrylate, and hexyl acrylate were all calculated to be 2 MPa. The range of elastic moduli could be further extended higher by incorporation of high glass transition monomers, such as methyl methacrylate, norbornene, or styrene, which are capable of free radical polymerization.

Blends of SIA 0210 and butyl acrylate, containing 3% (w/w) of a 1:1 mixture of Irgacure 819 and Irgacure 184 and 1% (w/w) SIB 1402, were cured with ultraviolet light under either a quartz template or a poly(ethylene) sheet to obtain thin crosslinked films on the order of 1–10 μm thick. Figure 3 shows the moduli calculated from force versus distance data for the set of SIA 0210-butyl acrylate blends. The modulus of the film increases linearly with the percent of SIA 0210. The modulus of the SIA 0210, the etch barrier, and *n*-butyl acrylate were calculated at 7.7, 4.2, and 2.1 MPa, respectively.

The pattern simulation was performed to determine whether catastrophic errors in pattern placement would result from the densification of the etch barrier. The reference model incorporated an elastic modulus of 1.6 MPa, a 10% (v/v) densification, and a Poisson's ratio of 0.3. A horizontal

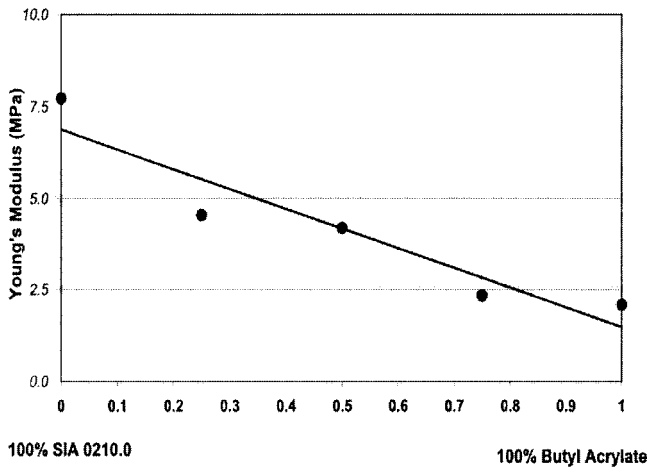


Fig. 3. Elastic moduli of butyl acrylate—3-acryoxypropyl tris(trimethylsiloxane)silane solutions.

cross section of the “in-plane” displacement magnitude was taken just above the feature base. The color-coded image of the in-plane pattern motion is shown in Fig. 4. The key point of interest is the movement of the line as it runs across the $2\ \mu\text{m} \times 2\ \mu\text{m}$ blocks in the pattern. The “in-plane” displacement of the line was found to be less than 1 nm. A simulation using another FEM package, COSMOS[®], corroborated this result. Both simulations predict that there will be no local pattern density effect in the SFIL resulting from volumetric contraction of the etch barrier.

A set of simulations was performed on 500 nm wide features, 200 nm tall features on a 100 nm base layer with a Poisson’s ratio of 0.5. The modulus ranged from 1 MPa to 1 GPa. The simulations revealed that the tensile modulus of the photopolymerized material does not affect feature shape. Densification fixes the strain at the etch barrier–transfer layer interface; Poisson’s ratio dictates how the stress is translated in the direction normal to the applied strain. While the modulus may affect the separation process, it does not affect the feature profiles.

The influence of densification and Poisson’s ratio on the cross section of features with width ranging from 100 nm to 10 μm has been investigated. For the simulations, the verti-

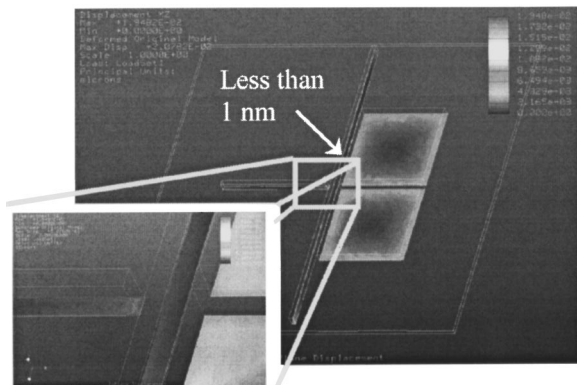
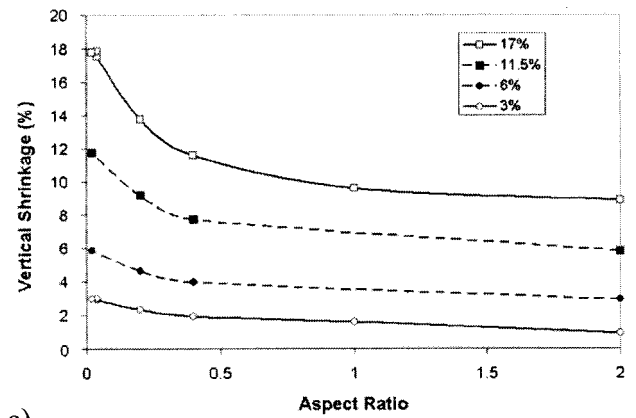
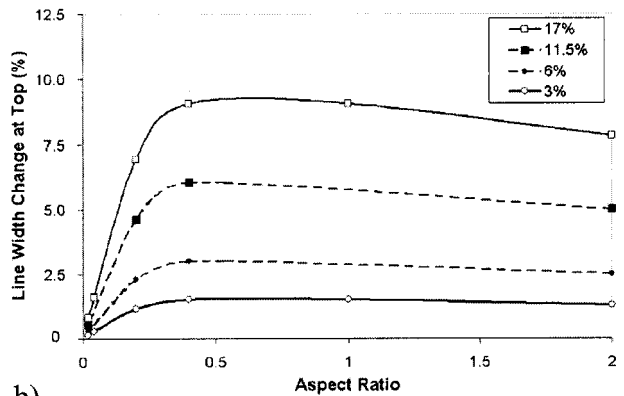


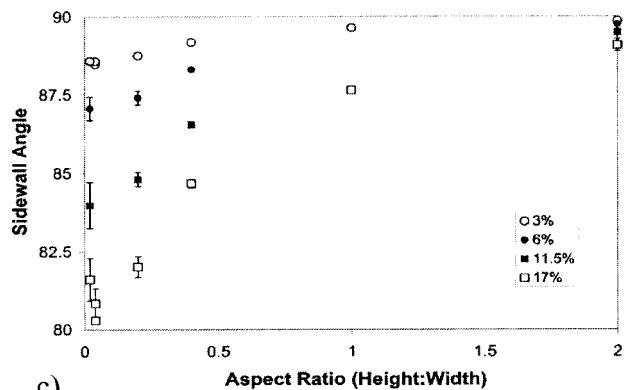
Fig. 4. In-plane motion of pattern (units are in microns).



a)



b)



c)

Fig. 5. (a) Vertical shrinkage of etch barrier features. (b) Effect of densification and Poisson’s ratio on linewidth shrinkage. (c) Effect of densification and Poisson’s ratio on sidewall angle.

cal shrinkage was measured from the center of the feature [point C in Fig. 1(b)] in a dense spacing. This height was subtracted from the average height of the feature base taken on the left [point E in Fig. 1(b)] and right side [point A in Fig. 1(b)]. The ratio of this height to the original height, 200 nm, is reported in Fig. 5(a). The densification of the monomer and the Poisson’s ratio both affect the vertical shrinkage significantly. The maximum vertical shrinkage predicted by the simulation is $\sim 17\%$ for a Poisson’s ratio of 0.5 and 17% densification. This maximum occurs in the center of the feature that experiences the greatest vertical shrinkage. This

point represents the worst-case scenario for the replication process.

The linewidth was measured at the top of the feature after densification and compared to the original width. The change in linewidth predicted by the simulation is shown in Fig. 5(b). The plot indicates that densification plays a major role in linewidth shrinkage. The percent change decreases as the features get wider but the absolute amount of linewidth change increases. In the worst case of 17% (v/v) densification, the actual distance at the top of the features that the linewidth changes approaches a limiting value of 80 nm for 200 nm tall features. The percent change in linewidth at the top of the feature associated with the densification is small; the worst case being 9.1% (or 20 nm of a 200 nm wide feature) for 17% densification and 0.5 Poisson's ratio. It should be noted that the linewidth change at the base of the features was computed and was less than 2.3% for even the worst case. For materials similar to the etch barrier (1 MPa, 8.9% densification, $\nu=0.4$), the linewidth change at the base of the feature was less than 0.3%.

The convolution of linewidth change and vertical shrinkage manifests itself in sidewall angle changes. Analysis of the resulting sidewall angle revealed a linear relationship with aspect ratio. Figure 5(c) shows that the sidewall angle is closer to 90° for smaller features than for larger features. The sidewall angle approaches 80° for small aspect ratio features with 17% densification and Poisson's ratio of 0.5. The line end angle was also studied as a function of aspect ratio; it follows a trend similar to that of sidewall to aspect ratio. As the aspect ratio becomes small, the difference between the sidewall angle and line end angle becomes very small.

IV. CONCLUSIONS

Photopolymerization of the acrylate systems used in SFIL are accompanied by volumetric contraction. This photopolymerization-induced densification is structure de-

pendent and can be tailored from 2% to 14%. The moduli of several prospective etch barrier monomers were obtained from Hertzian fits to AFM force–distance data. The modulus of the etch barrier formulation is tunable over a range of 2–30 MPa with the current acrylate functionality.

FEM analysis predicts that pattern placement will not be a problem for the current etch barrier formulation. It also predicts that densification will manifest itself mainly in the direction normal to the substrate surface. Linewidth change is a small percentage of the original linewidth. Sidewall angle and line end angle are aspect ratio and material property dependent. The effect of densification will be most prominent in isolated trenches. The sidewall angle for the 10 μm feature is greater than 80° for densification less than 17% and greater than 85° for densification less than 6.0%. These are reasonable profiles to etch transfer into the transfer layer with minimal bias associated with the subsequent reactive ion etch. We are now engaged in experiments designed to test these predictions.

ACKNOWLEDGMENTS

The authors appreciate the continued support of DARPA (Contract No. MDA972-97-1-0010) and SRC (Contract No. 96-LC-460). They extend special thanks to Larry Fire from PTC for the donation of Pro/E and Pro/Mechanica. They would also like to thank Cindy Stowell, Lindsay Pell, and Professor Brian Korgel (UT-Austin) for their time and for the use of the AFM.

¹M. Colburn *et al.*, Proc. SPIE **3676**, 379 (1999).

²M. Colburn, A. Grot, M. Amistoso, B. J. Choi, T. Bailey, J. G. Ekerdt, S. V. Sreenivasan, J. Hollenhorst, and C. G. Willson, Proc. SPIE **3676**, 379 (2000).

³*User's Guide to AutoProbe CP* (Park Scientific Instruments, Sunnyvale, CA, 1998).

⁴H. J. Hertz, J. Reine Angew Math. **92**, 156 (1882).

⁵I. N. Sneddon, Int. J. Eng. Sci. **2**, 47 (1965).

⁶K. L. Johnson, *Contact Mechanics* (Cambridge University Press, Cambridge, 1987).